



# On the role of meniscus geometry in capillary wave generation

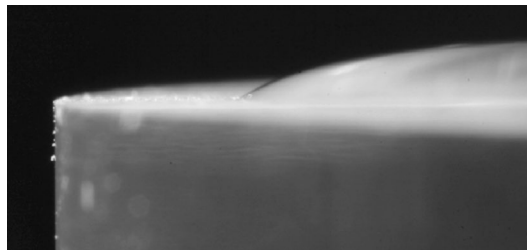
X. Shao<sup>1</sup> · C. T. Gabbard<sup>1</sup> · J. B. Bostwick<sup>1</sup> · J. R. Saylor<sup>1</sup>

Received: 14 December 2020 / Revised: 19 January 2021 / Accepted: 4 February 2021 / Published online: 1 March 2021  
© The Author(s), under exclusive licence to Springer-Verlag GmbH, DE part of Springer Nature 2021

## Abstract

Capillary waves, surface waves whose restoring force is dominated by surface tension, have been an important part of experimental fluid mechanics for many years. Capillary waves are typically generated by a vibrating wave generator which may be the walls of the tank containing the liquid or a separate object. In both cases, a meniscus exists at the interface between the liquid and the wave generator. Though this meniscus is due to the same surface tension that controls capillary waves, its effect on capillary wave formation has not been studied. Herein we present experimental results showing that such a meniscus is needed to form capillary waves, that the lack of a meniscus (a flat interface at the wall) prevents the formation of these waves, and that a meniscus of either positive or negative curvature serves equally well in enabling capillary wave formation.

## Graphic abstract



## 1 Introduction

Capillary waves have been the subject of experimental study for many years, with early analytic work of researchers such as Crapper (1957), quickly followed by experiments and field studies (e.g., Schooley 1958; Cox 1958). Capillary waves play a critical role in several aspects of oceanography and limnology. Specifically, they enhance the transport of heat and dissolved gases across the air/water interface of lakes and oceans (Witting 1971; Coantic 1986; Szeri 1997; Saylor and Handler 1997; Saylor 1999). They are also important in that they provide a means for momentum transfer from wind to waves and are the initial wave form that is observed on a calm surface when increasing wind develops a wave field (Hwang et al. 1996).

In the laboratory, capillary waves are typically generated in one of two ways, either (1) through the Faraday instability wherein a tank, vertically vibrated at an amplitude above a certain threshold, results in a wave field having a frequency that is usually one-half the driving frequency (Faraday 1831) or (2) via a wave generator. The latter is the focus of this work and occurs when a vertical wire or horizontal object located at the air/water interface serves as a wave generator or when a tank is vertically vibrated at an amplitude below the threshold for generation of Faraday waves. In the experiments presented here, we consider waves formed by the vibrating tank, but in both cases the waves emanate from a meniscus.

The meniscus that forms at either the tank wall or at the wave generator can be variable in its geometry. For example, when generating waves in a tank where the air/water interface is pinned at the tank rim (the case considered here), slight overfilling or underfilling of the tank changes the angle  $\delta$  of the air/water interface at the wall. This is illustrated in Fig. 1 where the tank is underfilled resulting in

✉ J. R. Saylor  
jsaylor@clemson.edu

<sup>1</sup> Clemson University, Clemson, SC, 29634, USA

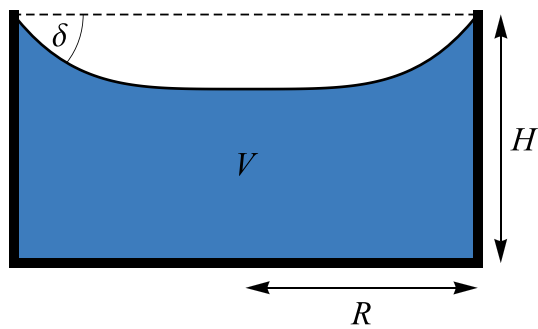


**Fig. 1** Illustration of meniscus geometry for a tank with a pinned air/water interface. The meniscus gives negative  $\delta$  for the underfilled condition and positive  $\delta$  for the overfilled or brimful condition

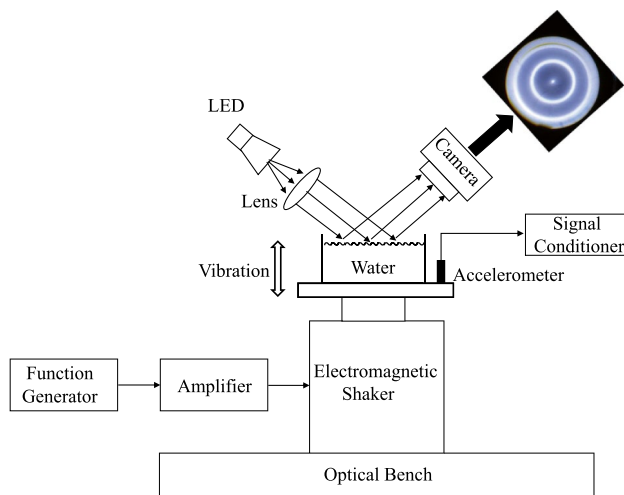


**Fig. 2** Experimental setup

$\delta < 0$ . The converse is an overfilled, or brimful tank, which gives a positive  $\delta$ .

Herein we present a set of experiments where edge waves are generated in a circular tank that is filled with a volume of water that spans the underfilled to overfilled condition ( $\delta$  attains negative and positive values) showing how the filling condition affects the wave field. The results show that an air/water interface without a meniscus (i.e.,  $\delta = 0$ ) is unable to generate edge waves and that such waves require nonzero  $\delta$ .

## 2 Experiment

The experimental setup used to study edge waves is presented in Fig. 2 and comprises a circular acrylic tank having a radius  $R = 35$  mm and depth  $H = 22$  mm (see also Fig. 1). The tank was mounted on a Labworks ET-139 electrodynamic shaker which provided vertical vibration of the tank. The shaker was driven by a Labworks PA-141 amplifier

modulated by an Agilent 33220A function generator. The tank motion was monitored using a PCB 352C33 accelerometer with a PCB 482C05 signal conditioner.

To characterize the capillary wave pattern, wave slope images were obtained using a collimated white light source and digital camera. Collimated white light was created using a white LED and a singlet lens having a 300 mm focal length. A plate with a 2-mm-diameter hole was placed in front of the light source and at the focal point of the lens. The resulting collimated light beam was directed at the wave surface, and the reflected beam was captured by a digital camera (Canon EOS Rebel T3i, with a Canon EF-S 18–55 mm lens) oriented so its optical axis coincided with that of the reflected, collimated beam. The angle between the vertical and the optical axes of the camera and the light source were the same. This setup yielded images that are bright at locations where the water surface is flat (at the wave peaks and troughs) and dark at locations where the water surface is tilted. The greater the tilt, the lower the pixel intensity, and so the greater the wave amplitude (at fixed wavelength), the lower the pixel intensities in the tilted regions of the wave field. A sample image is included in the inset of Fig. 2.

Here we are interested in waves under resonant conditions, i.e., where the waves emanate from the tank edge, propagate inward, and are reflected back at the geometric center to create a standing wave field. To find resonant conditions, excitation frequency sweeps were performed. The resonant condition was the frequency at which the images showed the greatest contrast between light and dark regions. This was because the camera exposure was long (1 s) ensuring that each image consisted of the integrated average of multiple wave periods. Under these conditions, only standing wave modes result in a clear pattern and frequencies at which traveling waves existed were blurred over, revealing little structure to the image. It should be noted that, though this method blurs over traveling waves in non-resonant conditions, once resonance is identified, traveling waves do not exist. Herein we studied the resonant condition which existed at a driving frequency of 11.2 Hz. For the results presented here, the amplitude of tank acceleration was on the order of  $0.5 \text{ m/s}^2$ .

Experiments were conducted for conditions where the tank was filled to the point where the water surface was flat and for conditions where the tank was over- or underfilled from this flat condition by + 2.0 ml, + 1.5 ml, + 1.0 ml, + 0.5 ml, - 0.5 ml, - 1.0 ml, and - 1.5 ml. Here a negative volume implies underfilling. Doubly distilled water was used for all experiments. The angle  $\delta$  for the overfilled cases was obtained from images obtained with a digital camera whose optical axis was parallel to the water surface and which passed by the edge of the meniscus. An example of such an image is presented in Fig. 3. Values for  $\delta$

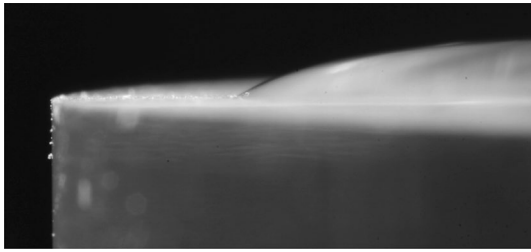


**Fig. 3** Image of meniscus for the case of 2.5 ml overfilling. The width of the tank wall (the flat region) is 3.1 mm in length

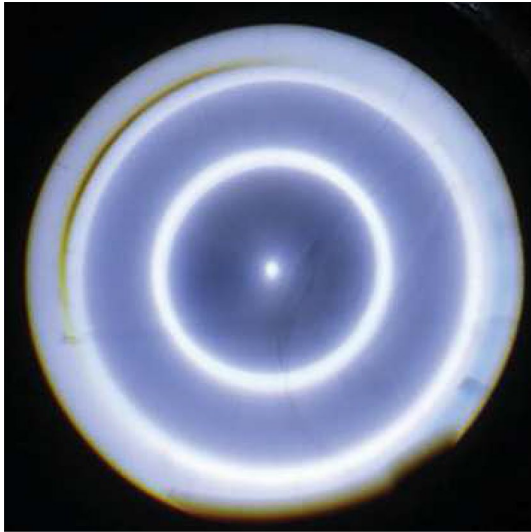


**Fig. 4** Typical wave slope image

were obtained from these images using the angle tool in the imageJ software package (Rasband 1997–2009), giving  $\delta = 4.6^\circ, 6.6^\circ, 10.1^\circ, 18.1^\circ, 20.2^\circ$  for 0.5 ml, 1.0 ml, 1.5 ml, 2.0 ml, and 2.5 ml, respectively. This approach was not feasible for the underfilled condition since it required imaging through the curved tank wall, a process which not only distorts the image, but results in variable distortion and defocussing as one moves radially inward from the inner surface of the tank wall. Accordingly we rely on symmetry for these underfilled conditions giving  $\delta = -4.6^\circ, -6.6^\circ, -10.1^\circ$  for the  $-0.5$  ml,  $-1.0$  ml, and  $-1.5$  ml cases, respectively.

### 3 Results and discussion

Figure 4 presents a sample wave slope image. Images such as these were azimuthally averaged to provide intensity versus radius profiles, and these are presented in Fig. 5 for all of the experimental conditions considered here. It is noted that the y-axis is light intensity in arbitrary units whose maximum value does not change significantly with the different under/

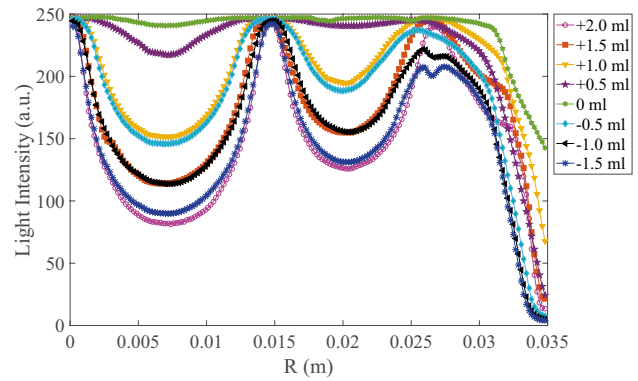


**Fig. 5** Plot of azimuthally averaged light intensity in arbitrary units versus radius, as it depends upon volume filling conditions,

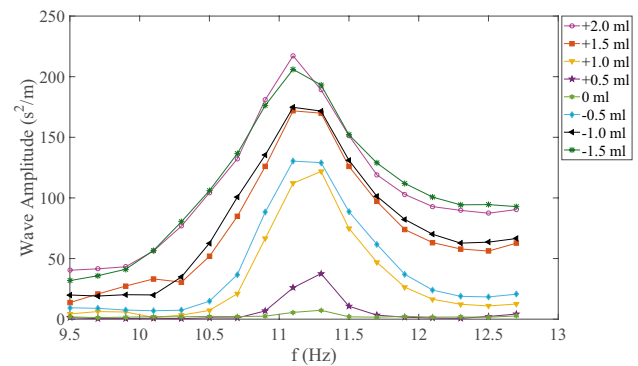


**Fig. 6** Frequency response diagram plotting a measure of wave amplitude against driving frequency for the  $n = 3$  mode, as it depends upon the volume filling conditions

overfilling cases. This is as expected since, regardless of the amplitude of the waves, the peaks and troughs will be horizontal and will reflect light, giving the maximum possible light intensity. In contrast, as the amplitude of the wave field increases, the slopes of the tilted regions become more extreme, and their light intensity gets progressively lower. Hence, the radial profiles in Fig. 5 will have minima that decrease with increasing wave amplitude. Consequently, the magnitude of the minima in this figure serves as a proxy for wave amplitude, and the difference between the first peak and first trough (for example) in these profiles is monotonically related to peak wave height. Accordingly, these profiles show that, first, a flat interface is effectively unable to produce edge waves and second that robust wave fields can be generated under either overfilled or underfilled conditions and that the greater the degree of over/underfilling, the greater the wave amplitude (the smaller the minima in the plot).

Figure 6 is a plot of the amplitude of the wave field versus the driving frequency for the range of under/overfilling conditions explored here. Our apparatus was not capable of

measuring the actual wave height, and so, here, the amplitude of the wave field is defined as the difference in the light intensity at the first maximum ( $R = 0$  m) and first minima ( $R = 0.007$  m) as seen in Fig. 5, divided by the measured acceleration. Scaling to the acceleration ensured that small variations in acceleration from run-to-run did not affect the plotted amplitude. Each of the frequency scans plotted here show a resonant condition at essentially the same frequency  $f = 11.2 \pm 0.1$  Hz, showing that the geometry of the meniscus does not materially affect the resonant condition.

Figures 5 and 6 show that the more over- or underfilled the tank, the higher the wave amplitude. The range of  $\delta$  explored here is the maximum attainable because further filling or emptying resulted in a de-pinning of the meniscus.

A mechanism explaining the necessity of a meniscus in order to generate capillary waves is now described. The curvature of the air/water interface at the edge of a container causes a pressure excess (positive or negative) depending on whether the curvature is concave or convex. At equilibrium, the sum of the gravitational head and the capillary pressure  $2\sigma/r$  creates at fixed depth a uniform pressure independent of radial location. Hence, for the overfilled geometry, the water in the center of the tank is higher than at the rim so that the gravitational head overcomes the overpressure due to the meniscus at the edge of the tank, whose concave side points toward the water, that overpressure equaling  $\rho g$  multiplied by the difference in the height of the air/water interface at the center and rim of the tank. The opposite is true for the underfilled case. When a tank is vibrated,  $g$  effectively becomes a time-varying value and the meniscus geometry must vary to accommodate the new value. The changing meniscus geometry is the oscillating change in the surface at the tank edge which causes waves to propagate. For the flat interface, the effective variation in  $g$  has no effect on the interface since the pressure beneath the interface remains independent of radial location at fixed depth, leading to the suppression of edge waves for this case, as observed experimentally.

#### 4 Concluding remarks

The study of capillary waves is an important part of experimental fluid mechanics, and herein we demonstrate the impact of meniscus geometry on one of the most common methods for capillary wave generation. The experimental result presented herein reveal that a tank must be either

overfilled or underfilled in order to generate capillary waves via vertical tank vibrations. Specifically, the greater the degree of under/overfilling, the greater the amplitude of a standing capillary wave field for a fixed amplitude of wave generator motion.

**Acknowledgements** JBB acknowledges support from NSF Grant CMMI-1935590.

**Authors' contribution** X.S. conducted the wave experiments, processed the data, and created the plots and most of the diagrams. C.T.G. obtained the images of the meniscus and measured the angle  $\delta$ . J.B.B. supervised the research and contributed to the writing of the paper. J.R.S. supervised the research, contributed to the writing, and oversaw the experiments.

#### Compliance with ethical standards

**Conflict of interest** The authors declare that they have no conflicts of interest.

#### References

- Coantic M (1986) A model of gas transfer across air–water interfaces with capillary waves. *J Geophys Res* 91:3925–3943
- Cox CS (1958) Measurements of slopes of high-frequency wind waves. *J Mar Res* 16:199–225
- Crapper GD (1957) An exact solution for progressive capillary waves of arbitrary amplitude. *J Fluid Mech* 2:532–540
- Faraday M (1831) On the forms and states assumed by fluids in contact with vibrating elastic surfaces. *Philos Trans R Soc Lond* 121:319–340
- Hwang PA, Atakturk S, Sletten MA, Trizna DB (1996) A study of wavenumber spectra of short water waves in the ocean. *J Phys Oceanogr* 26:1266–1285
- Rasband WS (1997–2009) ImageJ. National Institutes of Health, Bethesda
- Saylor JR (1999) The role of capillary waves in oceanic air/water gas exchange. *Tellus* 51B:616–628
- Saylor JR, Handler RA (1997) Gas transport across an air/water interface populated with capillary waves. *Phys Fluids* 9:2529–2541
- Schooley AH (1958) Profiles of wind-created water waves in the capillary-gravity transition region. *J Mar Res* 16:100–108
- Szeri AJ (1997) Capillary waves and air–sea gas transfer. *J Fluid Mech* 332:341–358
- Witting J (1971) Effects of plane progressive irrotational waves on thermal boundary layers. *J Fluid Mech* 50:321–334

**Publisher's Note** Springer Nature remains neutral with regard to jurisdictional claims in published maps and institutional affiliations.